Absorption, Photoluminescence, and Polarized Raman Spectra of a Fourfold Alkoxy–Substituted Phthalocyanine Liquid Crystal

7 AUTHORS, INCLUDING:

Elisabetta Venuti
University of Bologna
95 PUBLICATIONS **1,947** CITATIONS

SEE PROFILE

Ivano Bilotti
University of Bologna
26 PUBLICATIONS **406** CITATIONS

SEE PROFILE

Massimiliano Cavallini
Italian National Research Council
144 PUBLICATIONS **4,319** CITATIONS

SEE PROFILE

Annalisa Calò
IBEC Institute for Bioengineering of Catalonia
13 PUBLICATIONS **129** CITATIONS

SEE PROFILE

Absorption, Photoluminescence, and Polarized Raman Spectra of a Fourfold Alkoxy-Substituted Phthalocyanine Liquid Crystal

Elisabetta Venuti,*,† Raffaele Guido Della Valle,† Ivano Bilotti,† Aldo Brillante,† Massimiliano Cavallini,‡ Annalisa Calò,‡ and Yves H. Geerts§

†Dipartimento di Chimica Fisica e Inorganica and INSTM-UdR Bologna, Università di Bologna, Viale Risorgimento 4, I-40136 Bologna, Italy

‡CNR Institute for the Study of Nanostructured Materials, Via P. Gobetti 101, I-40129 Bologna, Italy

§Laboratoire de Chimie des Polymères, Université Libre de Bruxelles, CP 206/1 Boulevard du Triomphe, BE-1050 Bruxelles, Belgium

S *Supporting Information*

ABSTRACT: Absorption, photoluminescence, and Raman scattering measurements have been performed on a fourfold alkoxy-substituted phthalocyanine in solution and in the discotic liquid crystal phase. As already known for this class of compounds, the features of the electronic spectra in the condensed state are determined by the spatial closeness and arrangement of the π systems of the phthalocyanine cores, with the occurrence of collectively excited states and excimer-like emission. Quantitative information about the alignment of the molecules which compose the liquid crystal phase has been obtained from the analysis of polarized Raman spectra of homeotropically aligned samples.
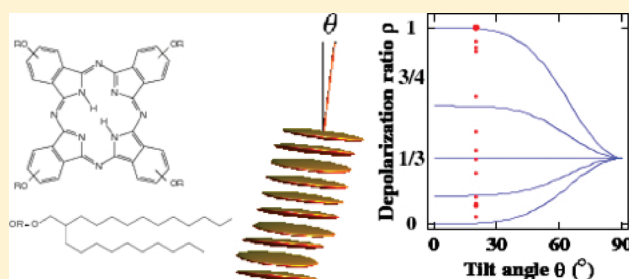
■ INTRODUCTION

Phthalocyanines derivatives, formed by a rigid aromatic core with long flexible chain substituents, are known to display discotic liquid crystalline (DLC) phases. At a supramolecular level these systems can be represented as columnar stacks with the rigid cores piled up and separated laterally by the long chains, so to make possible quasi one-dimensional transport behavior of both charge and excitation.[1−5] Hole mobilities of $0.1-0.5$ cm^2/(V s) have been measured[6] along columns where a good overlap of the molecular core π orbitals is achieved thanks to an optimal cofacial stacking in the conductive pathway.

DLCs are thus systems of increasing technological importance[7,8] as active layers in organic electronic and optoelectronic devices, such as field-effects transistors (OFETs), photovoltaics (OPVs), and light-emitting diodes (OLEDs). The kind of alignment of the columnar stacks is of crucial importance in devices. Two typical arrangements of DLCs with respect to the substrate are known: planar (or homogeneous) and homeotropic. In the former the columns are parallel to the substrate; that is, the disks lie perpendicular to it, as needed in OFETs. In the latter, instead, the columns are perpendicular to the substrate, with the disks roughly lying flat on the surface, as needed in OPVs or OLEDs.[2,6]

Homeotropic alignment can be achieved in thick films ($\approx$500 nm) of the metal-free fourfold alkoxy-substituted phthalocyanine[1,6,9] 2(3),9(10),16(17),23(24)-tetra(2-decyltetradeciloxy)phthalocyanine reported in Figure 1 (abbreviated H$_2$Pc1410),[10] by slowly cooling the melt confined between two substrates. As indicated by XRD,[1,9] H$_2$Pc1410 exhibits a columnar rectangular mesophase Col$_r$ up to 60 °C,[1,6,9,11] followed by the transition to a columnar hexagonal mesophase Col$_h$ which is the phase stable up to the melting temperature (180 °C).[1,6,12] The alignment properties in both phases have been studied by polarized optical microscopy[1,6,11] and AFM.[6] UV−vis absorption spectroscopy in the condensed phase has detected the hypsochromic shift associated with the formation of the so-called H-aggregates,[13] confirming a plane-to-plane columnar stacking of the molecules. In fact, the electronic spectroscopic behavior of phthalocyanine aggregates has been largely explained by the simple approach of the exciton theory in the point dipole approximation.[13,14] In this approach the flat core of the molecule is regarded as a point dipole, and the aggregates are approximated by collections of dimers. Thus, the excitonic state of a molecular dimer splits into two levels through the interactions between a pair of dipoles. Albeit approximate,[15,16] the theory describes satisfactorily some spectroscopy features, such as the above-mentioned absorption blue shifts and the lack of fluorescence, both typical of the cofacial H-aggregates.[17] In a *clamshell* arrangement, in which the phthalocyanine disks are not parallel but the molecules still lie one on top of the other, the theory predicts[17] a relaxation of the selection rules for the optical transitions. Both red and blue shifts can therefore be detected in absorption, while a red-shifted emission is
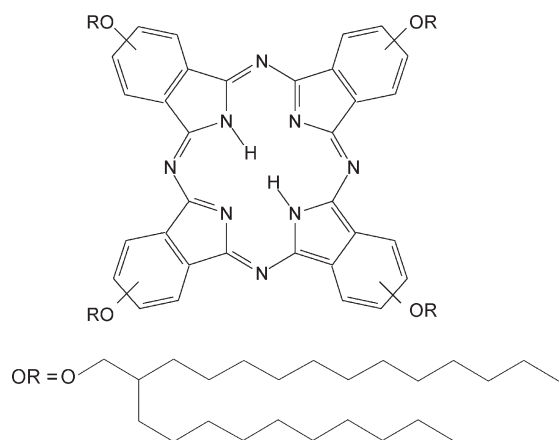
Figure 1. Chemical structure of the fourfold alkoxy-substituted phthalocyanine $H_2Pc1410$ under study.

Figure 2. Absorption spectra of $H_2Pc1410$ in CCl_4 solution and in the Col_r liquid crystal phase (smooth traces, as indicated). Excitation spectrum in the liquid crystal phase (noisy trace). Inset: geometry of the H_2Pc molecule. C, H, and N atoms are indicated in black, white, and midtone. Molecular graphics by MOLSCRIPT.[29]

not ruled out. In any case, the formation of stacked aggregates of phthalocyanine in the condensed state is accompanied by an emission quantum yield of orders of magnitude lower than that of the monomeric species in solution.[18] This also means that, despite the fact that DLC phthalocyanines absorb light virtually over the entire visible range,[19] the detection of the Raman scattering becomes possible.

In this work we address the study of the absorption, luminescence, and polarized Raman spectroscopic properties of $H_2Pc1410$ LC homeotropic films deposited on silica oxide, with the goal of better understanding the alignment features and to check if Raman spectroscopy could efficiently be used to probe such an alignment. Experimental observations are supported by DFT calculations which allow us to assign the Raman spectrum and by a theoretical analysis of the band intensities of the polarized spectra in light of the orientation of the film.

■ THEORETICAL METHODS

Raman Frequencies and Intensities. Harmonic vibrational eigenvectors and eigenvalues of unsubstituted phthalocyanine H_2Pc were calculated by standard ab initio methods with the Gaussian03 program,[20] using the B3LYP exchange correlation functional combined with the 6-31G(d) basis set.[20−22] As recommended for this combination,[23] the standard scaling of 0.9613 was applied to the vibrational frequencies. Subsequently, four short alkoxy substituents (either O-methyl or O-ethyl) were introduced in the β positions of the benzene rings so to obtain all the possible topological symmetries (namely D_{2h}, C_s, C_{2v}, and C_{4h}). This allowed us to check whether the presence of the alkoxy groups, along with the symmetry lowering, could affect the calculated frequencies of the modes which characterize the vibrational spectrum of H_2Pc . As further discussed in the section titled Raman Spectra, the eigenvalue and eigenvector analysis proved that the substitutions have very little effect on the character, the frequencies, and the intensities of modes localized on the flat disk of the molecules. As the ab initio modeling of the long side chains of $H_2Pc1410$ would require much useless computational efforts, assignments and discussion of the Raman spectra can be made assuming the parent H_2Pc as the model system. The frequencies ν_s of the intramolecular vibrations and their Raman intensities in the gas phase are therefore calculated at the geometry of minimum energy for the isolated H_2Pc molecule, which has D_{2h}
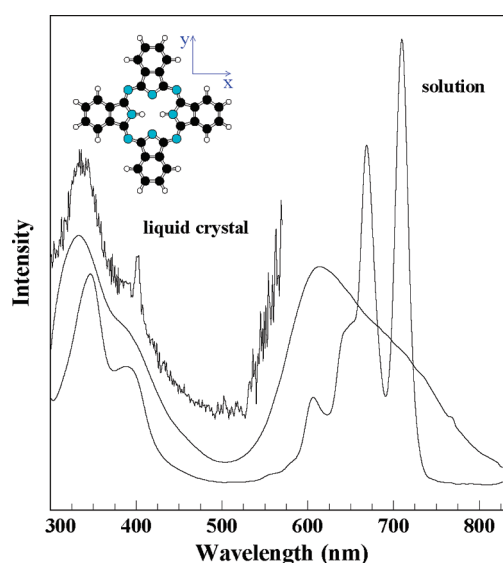
symmetry and is drawn in the inset of Figure 2. The molecule lies on the xy plane, with the two NH groups on the x axis.

Depending on the orientation of the molecule and on the polarization of the light beams, the Raman intensities[24] for a given mode s are controlled by various components of the derivatives α^s of the polarizability α with respect to the normal coordinate q_s. Here α^s is a symmetric 3×3 matrix, with components $\alpha_{ij}^s = \alpha_{ji}^s$. The indices i and j run on Cartesian components (x,y,z), while s indicates the normal mode. For a D_{2h} molecule, only intramolecular modes of symmetry species a_g, b_{1g}, b_{2g}, and b_{3g} can be Raman active.[25] Only components α_{xx}, α_{yy}, and α_{zz} are allowed to be nonzero for a_g modes, and only α_{yz}, α_{xz}, or α_{xy} for b_{1g}, b_{2g}, or b_{3g}, respectively.

For a large planar molecule such as H_2Pc, it is plausible to find large systematic intensity differences between in-plane (a_g or b_{3g}) and out-of-plane vibrations (b_{1g} or b_{2g}), since computed in-plane polarizabilities are much larger than out-of-plane polarizabilities. Polarizability components α_{yz} or α_{xz} (for b_{1g} or b_{2g} modes, respectively) are negligible with respect to α_{xy} (for b_{3g}). For a_g modes, α_{zz} is negligible with respect to α_{xx} and α_{yy}.

Raman Depolarization Ratios. Polarized Raman spectra on oriented molecules probe single α_{ij} components, while less ordered situations involve appropriate combinations of α_{ij}s. Therefore, the polarized spectra can be used to obtain information about the orientation of the molecules. To extract this information from the experiments, we need to transform the polarizability derivatives α^s from the molecular reference frame (x,y,z) to the laboratory frame (X,Y,Z). The laser is assumed to travel along the Z axis and is polarized on the X axis of the *laboratory frame*; the substrate surface lies on the XY plane orthogonal to the beam; the Raman radiation collected in a backscattering geometry is analyzed with a polarizer on either the X or Y axis (parallel or perpendicular to the exciting polarization), yielding intensities $I_\| = I_{XX}$ or $I_\perp = I_{XY}$.

As already mentioned, the molecular plane has been chosen as the xy plane of the molecular frame. The molecule-to-laboratory

rotation matrix is a well-known[26,27] function $\mathbf{R}(\psi,\theta,\phi)$ of the Euler angles ψ, θ, and ϕ. Following the standard convention,[26] θ is the angle between Z and z (i.e., tilt between normal-to-substrate and molecular axis); ψ describes the rotation of the molecule around its z axis; ϕ describes its rotation around the laboratory Z axis. The polarizability derivatives $\boldsymbol{\alpha}^s$ can be transformed to the laboratory frame as $\tilde{\boldsymbol{\alpha}}^s = \mathbf{R}\boldsymbol{\alpha}^s\mathbf{R}^\dagger$. The Raman intensity with input and output polarizers along the axes i and j is proportional to $I^s_{ij} = F(\nu_0,\nu_s,T)(\tilde{\alpha}^s_{ij})^2$. Here ν_0, ν_s, and T are frequency of the exciting radiation, the vibrational frequency, and the temperature. For the Stokes component of the Raman spectra (emitted at frequency $\nu_0 - \nu_s$), $F(\nu_0,\nu_s,T) = (\nu_0 - \nu_s)^4/[\nu_s(1 - \exp(-h\nu_s/k_B T))]$.[24,28] The weight function $F(\nu_0,\nu_s,T)$ does affect the spectra but cancels out while computing the depolarization ratios $\rho = I_\perp/I_\parallel$.

Once given the distribution of the orientation angles ψ, θ, ϕ, appropriate angular averages yield the Raman intensities $I_\perp = I^s_{XY}$ and $I_\parallel = I^s_{XX}$, and thus the ratio ρ. The common case of a complete orientational disorder, for example, involves an average over all possible orientations in the three dimensions and thus follows the same rules as for liquids and gases.[24,25] In this case, for non-total-symmetric modes, the depolarization ratio is always $\rho = 3/4$, while for total-symmetric a_g modes, one finds $0 \leq \rho \leq 3/4$. The case appropriate to the columnar homeotropic phases studied in this work is discussed in section Polarized Raman Spectra.

■ EXPERIMENTAL METHODS

For the measurements on the liquid crystal phase, thick films were prepared by depositing $1-2$ mg of $H_2Pc1410$ between two glass plates. The glasses were first cleaned by dipping them in isopropanol and pure acetone and then drying with nitrogen. Then they were dipped in HF solution 4% for 5 s, washed with UHQ water, and finally dried. The sample was heated from RT to 183 °C at the rate of 10 °C/min in a controlled atmosphere ($p = 0.1$ mbar) using a heating stage Linkham THMS600. At this temperature, the film melts and becomes dark under polarized optical microscope. Subsequently the film was slowly cooled down to 178 °C. We verified that the film remains dark and no birefringent textures appear, except for defects which, as reported in the literature,[6] appear as straight birefringent lines. At this point the film was cooled to room temperature by shutting down the heating stage.

Absorption spectra were recorded with a CD Jasco J500A spectropolarimeter. Raman spectra were collected using a single grating spectrograph Renishaw System 1000 equipped with a suitable notch filter and a CCD detector. Raman scattering was excited with a Ar$^+$ laser at a wavelength of 514 nm and a spectral resolution of 3 cm^{-1}; the laser output power of 25 mW was reduced by means of neutral optical filters (from 50% to 90%) to avoid thermal damage of the sample. By using a $50\times$ objective, a laser spatial resolution of about 0.8 μm was reached. A linear background subtraction was applied when necessary. Photoluminescence measurements (PL), both for solutions and liquid crystal homeotropic samples, were performed with the same experimental setup as the Raman experiments. Excitation wavelength from the Ar$^+$ laser at 514.5 nm, focused, or from a diode laser at 404 nm, unfocused, gave essentially the same photoluminescence profiles. We therefore decided to use the laser at 514.5 nm so to fully exploit the confocality of the spectrometer. PL and excitation spectra were also recorded with a FLSP920 Spectrometer by Edinburgh Instruments, equipped with a 450

xenon arc lamp, single emission and excitation monochromators, and a Peltier cooled Hamamatsu R928P photomultiplier. Standard filters at suitable wavelengths were used to cutoff scattered light. The CCl_4 solvent from Fluka used for the measurements in solution was of spectroscopic grade.

Measurements on samples obtained after separating the two glass plates confirmed that, from a spectroscopical point of view, these performed identically to the original films. However, they generally showed a faster degradation upon irradiation at 514.5 nm.

■ RESULTS AND DISCUSSION

Absorption Spectra. Electronic spectra of phthalocyanines originate from the extended conjugated aromatic system of the core-disk, which acts as a very effective chromophore. Their absorption spectra have been extensively studied and described,[5] and it is just worth mentioning that systems with a core-disk having D_{2h} symmetry, such as the metal-free unsubstituted phthlocyanine H_2Pc and the $H_2Pc1410$ under study, display two strong ($\pi-\pi^*$) absorptions in the red range of the visible electromagnetic spectrum. These correspond to transitions polarized either along the x or the y molecular axes, known as Q_x and Q_y bands. These bands are responsible for the strong colors of all phthalocyanines, and in H_2Pc diluted toluene solutions[30] occur at 655 and 695 nm, respectively. At higher energy, around 350 nm, the B band, also known as Soret band, appears. In the condensed state, both Q and B bands broaden and partly overlap, and in fact crystal and liquid crystal phthalocyanines absorb light throughout the entire visible region of the electromagnetic spectrum.[19]

Absorption spectra of $H_2Pc1410$ in 10^{-6} mol/L CCl_4 solutions and in the Col_r liquid crystal phase are shown in Figure 2. Electron donating substituents like alkoxy groups in β (meta) positions on the benzene rings do not perturb strongly the Q_x and Q_y maxima,[5] nor the B band, and only minor red shifts with respect to the H_2Pc spectrum are usually expected. This is certainly the case with $H_2Pc1410$ in CCl_4 solutions (Figure 2), for which we observe two main maxima at 671 and 711 nm for the Q_x and Q_y transitions, respectively, with a red shift of only 16 nm with respect to the H_2Pc spectrum.[30] A comparison with the values of 666 and 703 nm, reported for the fourfold substituted β(OBu)-H_2Pc in diluted solutions,[31] also shows how the length and the ramification of the substituents play a very minor role.

In the Col_r liquid crystal phase of $H_2Pc1410$, the absorption spectrum broadens significantly and the maximum appears blue-shifted (Figure 2). By deconvolution the band can be solved in two main contributions, at 608 and 688 nm. A long tail on the red side reaches down to about 800 nm. It should be noted that the split between the Q_x and the Q_y bands appears considerably larger than in the solution. All these features are recognizable signatures of the formation of H-aggregates[1] and therefore of strong intermolecular interactions.[1,32,33] It is worthwhile to compare the absorption spectrum of the liquid crystal phase to the spectra of H_2Pc crystalline films.[34] Two crystal phases are known,[34,35] α- and β-H_2Pc. They exhibit similar herringbone structures, where the molecules are arranged in columnar stacks with a distance of 3.4 Å between the molecular planes. The two phases differ mainly for the tilt angle θ' between molecular and stacking axes, 26.5° for the α form and 46.8° for the β form.[35] The characteristics of the condensed state spectrum are expected to be determined by the interactions between neighboring
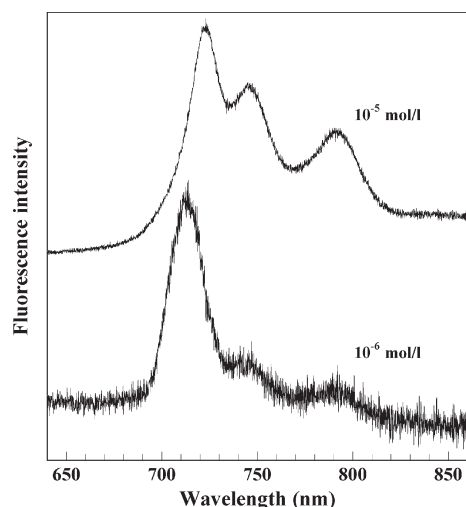
12152

dx.doi.org/10.1021/jp202926j |*J. Phys. Chem. C* 2011, 115, 12150–12157

Figure 3. Fluorescence spectra of $H_2Pc1410$ in CCl_4 solutions, at concentrations 10^{-5} and 10^{-6} mol/L.

Figure 4. Fluorescence spectra of a homeotropically aligned $H_2Pc1410$ liquid crystal sample. Three spectra (labeled 1, 2, and 3) are consecutively recorded on the same spot.

molecules in a column, and one can expect that the spectral features will be similar if column characteristics and molecular spacings are basically retained.[36] Since the absorption spectrum of $H_2Pc1410$ liquid crystal (Figure 2) is very close to the published spectrum of α-H_2Pc films[34] and completely different from that of β-H_2Pc,[34] the arrangement of the phthalocyanine core-disks in $H_2Pc1410$ must resemble that in α-H_2Pc films.[34] In the Col_r columnar rectangular phase of the $H_2Pc1410$ liquid crystal the stacking distance, in fact, is[1] 3.4 Å like in the crystal, and the tilt angle θ' is[1,9] around 15°.

Unlike the crystal, rotational angles and relative shifts between neighboring molecules are variable in the mesophase, so that this phase is characterized by a much larger degree of disorder. Numerical calculations[16] performed to determine the energies of Frenkel excitons in columnar mesophases have proved that in systems with two nondegenerate electronic transitions polarized on the molecular plane, a large broadening of the absorption spectrum is expected in the presence of rotationally disordered aggregates with a distribution of shifts between the molecular planes. This arises naturally from the fact that when the relative angles of the molecular planes are at random, many relative configurations of the transition dipoles can be sampled, and a full range of energies can be probed, while the eigenstates of the system are in fact built on both molecular transitions.[16]

Photoluminescence Spectra. The intrinsic fluorescence quantum yield of phthalocyanines is very high, and a radiative emission can be observed even when the excitation is far from the absorption maximum. However, the actual yield is expected to depend dramatically on the state of aggregation, and in the presence of the H-aggregates formed by the stacking of molecules, emission should be absent.

Fluorescence spectra of $H_2Pc1410$ in CCl_4 are shown in Figure 3. In diluted solutions ($\approx 10^{-6}$ mol/L) and at the excitation wavelength of 514 nm, the deconvolution of the emission spectrum of $H_2Pc1410$ yields an intense band at 711 nm, with a weak shoulder near 722 nm, and two more bands of comparable intensities at 745 and 790 nm. By analogy with the assignments made for H_2Pc,[30] the 712 nm band, observed in a concentration regime where no aggregation should take place, is readily assigned to the single molecule (0−0) emission
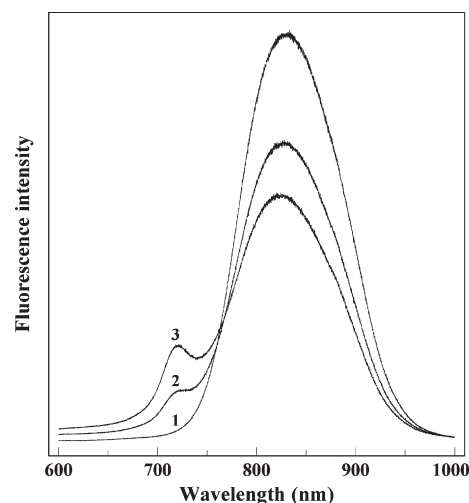
(monomeric), while the shoulders on the red probably involve radiative decay processes on vibrationally excited states.

By increasing the concentration by 1 order of magnitude ($\approx 10^{-5}$ mol/L), the relative intensity of the band at 712 nm strongly decreases compared to those of the bands at 745 and 791 nm. This can readily be attributed to reabsorption of the Q_y transition.

In the homeotropically aligned liquid crystal samples at room temperature, we have observed a very broad weak emission (trace 1 of Figure 4), roughly centered around 840 nm, which cannot be fitted by a single band. The global fit of the emission spectra yields two main broad emissions, centered around 803 and 860 nm, with varying relative intensities. It is worth noticing that both homogeneous samples and pristine material at room temperature display the same emission spectra. To check the origin of this emission, and confirm that the genuine fluorescence of $H_2Pc1410$ has been observed, the excitation spectrum at 810 nm was recorded (Figure 2). As can be seen, in the excitation spectrum the B band characteristic of the condensed absorption spectrum is faithfully reproduced, while the Q band detection is made more cumbersome by scattered light.

The general features of the emission spectrum of $H_2Pc1410$ can be interpreted as typical of multiple radiative deactivation of families of excited molecules organized in stacks, with an excimer-like character. The occurrence of many possible different relative arrangements of molecule pairs, including those that can be described as clamshell ones, determines a relaxation of the selection rules of the exciton theory, and the appearance of the red-shifted emission.

The observed emission is similar to that reported both in the crystal state and in films of metal-free phthalocyanines[34,37] and for octa-alkoxy substituted phthalocyanines in the liquid crystal state.[37] In the latter case[37−39] the mesophase showed a dramatic drop of emission quantum yield with respect to the crystal, whereas no remarkable differences were found between their emission spectra.

While detecting the fluorescence, we also noticed that when the laser power threshold was set higher than the 10% of its full value (25 mW), a narrow band centered at 718 nm developed, whose intensity kept growing with the time of irradiation, as
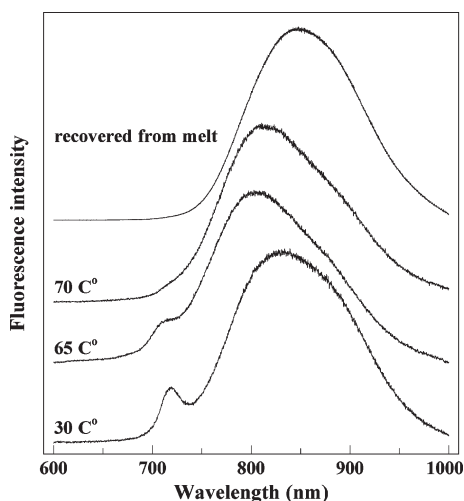
12153

dx.doi.org/10.1021/jp202926j |*J. Phys. Chem. C* 2011, 115, 12150–12157

Figure 5. Fluorescence spectra of a homeotropically aligned $H_2Pc1410$ liquid crystal sample as a function of temperature across the Col_r to Col_h transition.

Figure 6. Experimental *unpolarized* Raman spectra of $H_2Pc1410$ in the Col_r phase, and calculated spectra for H_2Pc and for a 1:4:2:1 mixture of the four β(O-met)-H_2Pc isomers with symmetry D_{2h}, C_s, C_{2v}, and C_{4h}.

shown in Figure 4. The phenomenon did not appear to be spontaneously reversible, since the 718 nm emission could be collected with the same intensity after keeping the sample in the dark. The spectral change was not matched by any detectable morphological change observable by the optical microscope of the apparatus.

The sample was subsequently placed on the heating stage. At 30 °C, under irradiation, the emission at 718 nm appeared, as expected. The temperature of the entire film was subsequently gradually increased, while measurements were repeated at discrete temperatures on the same spot, keeping the laser intensity below the threshold of 10% of its full power. As can be seen from the spectra, shown in Figure 5, the 718 nm band becomes weaker across the phase transition from rectangular columnar Col_r to hexagonal columnar Col_h mesophase. At 70 °C, where the phase transformation has taken place, it has disappeared. The sample recovered at room temperature after melting does not show it either, behaving like a freshly prepared sample. Note also that the emission above 65 °C appears blue-shifted, but the deconvolution of the broad band system shows that it can be resolved in two or more bands whose maxima are still basically coincident with those of the low temperature phase.

Bandwidth and energy of this 718 nm emission nearly match those of the just mentioned monomeric emission, taking into account the solid state environment. Therefore the 718 nm emission must be interpreted as originating from excited isolated molecules, or less relaxed excimer states, probably generated by the disruption of the packing order of the Col_r mesophase as a consequence of the laser localized heating. The disappearance at temperatures higher than the phase transition suggests that the hexagonal phase has a sort of self-healing capability, probably due to higher thermal energy.

■ RAMAN SPECTRA

Confocal micro-Raman spectra of $H_2Pc1410$ have been recorded both on homeotropically aligned and edge-on samples in the wavenumber region 200−1800 cm^{-1} at the excitation wavelength of 514.5 nm (as reported in the section Experimental Methods). The broadening of Soret and Q bands in the
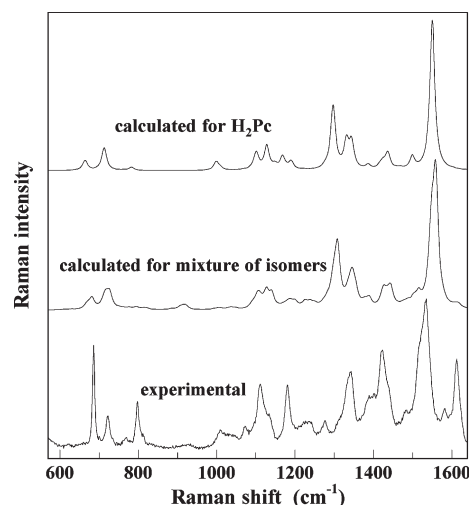
condensed phases, with the absorption occurring over the entire visible region of the electromagnetic spectrum,[19] has as a consequence that the Raman scattering exhibits resonance or preresonance enhancement due to interaction with either one or both of the electronic transitions.[19] Indeed, all the Raman spectra presented a sloping background due to the tail of the photoluminescence. The collection of Raman spectra at lower excitation energy (that is 647.1 nm) is in fact made extremely cumbersome by strong emission and reabsorption. The detailed analysis of the Raman spectra of $H_2Pc1410$ relies on a number of experimental and theoretical evidence and/or assumptions, as anticipated in the section Theoretical Methods. First, it is worth considering the spectrum calculated for the fourfold substituted β(O-met)-H_2Pc by assuming a mixture of the four isomers with topological symmetries D_{2h}, C_s, C_{2v}, and C_{4h} with the appropriate[1] statistical ratios 1:4:2:1. This spectrum, shown in Figure 6, must be compared both with the calculated spectrum of unsubstituted H_2Pc and with the experiment for $H_2Pc1410$, also shown. The comparison shows how the flat central system of the core-disk, with the in-plane vibrations, is responsible for all the major features of the vibrational spectrum, with no clearly detectable influence of the long aliphatic chains. The symmetry breaking induced by fourfold substitution on the phthalocyanine ring has minor effects on the overall spectrum but allows the modes of ungerade symmetry in the original D_{2h} skeleton of H_2Pc to become weakly Raman active. These modes are responsible for the very weak bands around 925 and 1230 cm^{-1}.

When moving to consider the crystal field effects, the factor group analysis, applied to the $c2mm$ 2D symmetry group of the $H_2Pc1410$ liquid crystal, reveals that the core-disk vibrations of the gerade in-plane modes of a_g and b_{3g} of the D_{2h} molecular group transform into modes of A_1 and A_2 symmetries, respectively, thus being still distinguishable in polarized Raman measurements. In other words, the Raman spectra of this liquid crystal can be fully interpreted on the basis of the known H_2Pc Raman spectrum in the solid phase.[40−43]

Keeping this in mind, the intense bands lying between 600 and 800 cm^{-1} can be readily assigned to the in-plane breathing vibrations and deformations of the central macrocycle. The spectrum between 1000 and 1230 cm^{-1} is expected to be
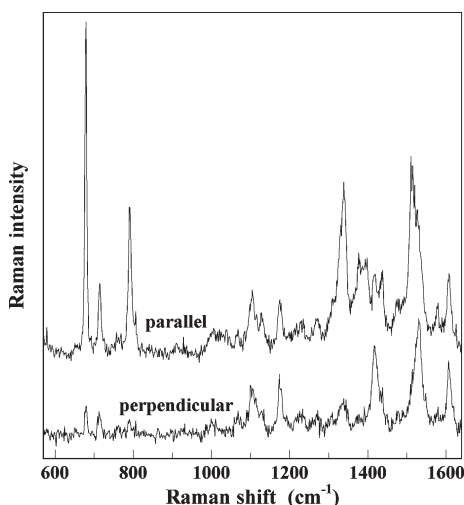
Figure 7. Raman spectra of homeotropically aligned $H_2Pc1410$ in the Col_r phase, analyzed with a polarizer parallel or perpendicular to the exciting polarization ($I_\parallel$ or $I_\perp$).

Figure 8. Lines: computed depolarization ratios $\rho = I_\perp/I_\parallel = \mathcal{R}(r,\theta)$ as a function of the tilt angle θ, for various values of the parameter r. Circles: experimental ratios ρ_s in the Col_r phase, drawn at the largest θ consistent with the experiments. Larger circles represent overlapping points, with an area proportional to the amount of overlap.

dominated by the many in-plane C—H bendings and deformations, with the exception of the band observed at 1134 cm^{-1} (1140 cm^{-1} in H_2Pc) that is mainly described as a pyrrole ring breathing. The strong band at 1342 cm^{-1} (1337 cm^{-1} in H_2Pc) arises from the scattering of the C_α—C_β stretching in the pyrrole units.[40,43] Finally, the 1500—1600 cm^{-1} range is characterized by two strong bands at 1513 and 1534 cm^{-1}, which are assigned to C—N pyrrole stretching and isoindole ring C—C stretching, respectively. The eigenvector analysis made on the ab initio results of β-substituted alkoxy phthalocyanines, with a much shorter aliphatic chain, supports all the assignments.

The experimental Raman intensities do not agree very well with the calculated intensities of Figure 6, obtained from the the ab initio scattering activities of the various bands. However, they match very well those observed in H_2Pc and other phthalocyanines[40,41,43] at the same excitation wavelength. This arises from the wavelength dependence of the relative intensities, as a consequence of the resonance or preresonant conditions of the Raman scattering, as previously mentioned. It has been shown, in fact, that the electron density involved in the Q band transition is localized on the inner part macrocycle, whereas the B band concerns the benzene rings, which are more peripheral. It is therefore possible to correlate the intensity profiles of the peaks with the excitation wavelength to the localization of the vibrational mode involved. For instance, the relatively strong intensity of the band at 1513 cm^{-1}, compared to the one at 1534 cm^{-1} at this excitation wavelength, is in contradiction with the calculated value. However, this proves that the 1513 cm^{-1} mode is more efficiently enhanced at wavelengths closer to the tail of the B band, thus confirming that the motion is mostly localized on the outermost part of the macrocycle.[40,43]

Raman spectra were also recorded at 65 °C, the transition temperature between phases Col_r and Col_h, but no significant spectral differences were observed.

All the normal modes previously mentioned concern motions in the plane of phthalocyanine disks, either of a_g or b_{3g} symmetry, and are therefore the most suitable candidates to probe the alignments of the molecules via polarization measurements.[44,45]

Polarized Raman Spectra. Polarized Raman spectra have been recorded for homeotropic samples in the Col_r phase. Figure 7 shows the spectra recorded with the exciting light
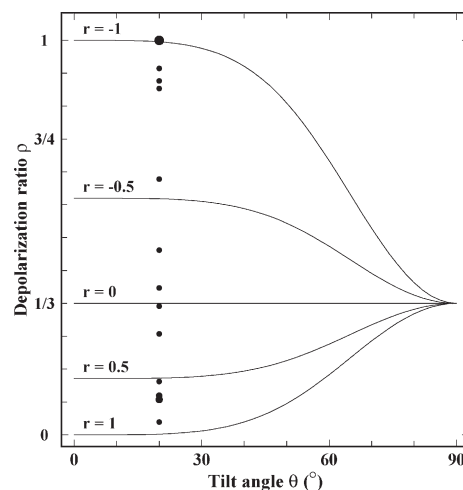
linearly polarized on the sample surface and analyzed in backscattering geometry either parallel ($I_\parallel$ spectra) or perpendicular ($I_\perp$ spectra) to the exciting polarization. All the samples showed a weak birefringence throughout the surface, which is an intrinsic property of the $c2mm$ rectangular columnar phase and can be observed by rotating the specimen under the polarizing microscope. Different domains can so be identified, which show extinction at different angles, indicating that the surface must be treated as polycrystalline. Although the area of these domains was within the spatial resolution of our spectrometer, we did not try to orient them singularly. Still, the polarized spectra can be used to draw some useful information about the alignment of the phase. For this purpose, we have fitted a set of Lorentian bands, plus a linear background, to the experimental spectra. Corresponding bands s in the parallel and perpendicular spectra received the same frequency ν_s and linewidths Γ_s, but independent intensities $I_\parallel^s$ and $I_\perp^s$, with a constraint $I_\perp^s \leq I_\parallel^s$. From the intensities obtained from the fit, we have computed the depolarization ratios $\rho^s = I_\perp^s/I_\parallel^s$, displayed in Figure 8.

We have finally checked the calibration of the instrument by repeating measurements and analysis for the T_2 symmetry band at 314 cm^{-1} of liquid CCl_4 and found $\rho = 0.75 \pm 0.04$, in perfect agreement with the expected value[25] for any non-total-symmetric band, $\rho = 3/4 = 0.75$. As already mentioned, this is also the maximum possible ratio for complete orientational disorder. For $H_2Pc1410$ we observe several ratios above 3/4, as shown in Figure 8. It is therefore evident that the experimental spectra are incompatible with a completely disordered sample. The depolarization ratios, therefore, contain information on the distribution of the molecular orientations with respect to the surface. This distribution depends on the orientations of the molecules with respect to the stacks and of the stacks with respect to the surface. The three angles, θ' (between molecular and stack axes), θ'' (between stack and normal to the surface), and θ (between molecular axis and normal to the surface), are constrained by $|\theta' - \theta''| \leq \theta \leq |\theta' + \theta''|$.

For the columnar homeotropic phases studied in this work, it may be safely assumed that the molecules can rotate around their

z axis and that all possible orientations around the laboratory Z axis are present in the polycrystalline XY surface. In this case $(\tilde{\alpha}_{ij}^{s})^2$ must be averaged over all possible values of ψ and ϕ $(0-2\pi)$. The resulting depolarization ratio $\rho = I_{\perp}/I_{\parallel}$ is a function of the tilt angle θ and of the nonzero polarizability derivatives $\tilde{\alpha}_{ij}^{s}$. The two cases of interest for H_2Pc are the in-plane vibrations of symmetry b_{3g} (only α_{xy} nonzero) and a_g (α_{xx} and α_{yy} nonzero, α_{zz} nonzero but negligible). We have computed the angular averages of our system, and thus the depolarization ratio ρ, with the symbolic algebra program Mathematica.[27,46] For modes of a_g symmetry, with $\alpha_{zz} = 0$, we find

$$\rho = \mathscr{R}(r,\theta) = \frac{1}{3} - \frac{32}{3}\frac{r}{3+r}\frac{\cos^2\theta}{3+2\cos^2\theta+3\cos^4\theta}$$

The parameter $r = 2a_{xx}a_{yy}/(a_{xx}^2 + a_{yy}^2)$, which depends only on the relative values of a_{xx} and a_{yy}, is $+1$ if a_{xx} and a_{yy} have identical magnitude and sign, -1 if they have identical magnitude but opposite sign, 0 if either a_{xx} or a_{yy} is zero. The depolarization ratio $\rho = \mathscr{R}(r,\theta)$ as a function of the angle θ, for various values of the parameter r, is shown in Figure 8. The range of possible depolarization ratios depends on the tilt angle θ, a fact that will enable us to deduce the angle from the experimental ratios. If θ is close to 0° (molecules lying flat on the substrate), all ratios ρ between 0 and 1 are possible. If $\theta = 90°$ (molecules normal to the substrate), $\rho = 1/3$ for all values of r. Intermediate angles correspond to appropriate ranges. For modes of b_{3g} symmetry, provided that α_{xy} is nonzero, we find $\rho = \mathscr{R}(-1,\theta)$. Depending on the angle θ, ρ goes from 1/3 to 1.

By referring to Figure 8, since the observed depolarization ratios are in the range $0.03-1.00$, we can deduce that the tilt angle θ is likely to be below 20° and that angles approaching 30°, or larger, are not consistent with the experiments. This result, which is the first *direct* constraint on θ, is consistent with the available information on θ' and θ''.

The analysis of the angular dispersion of the X-ray scattering intensity[9] yields a most probable θ' angle (between molecular and stack axes) around 15°. This value is in agreement with the results of recent MD simulations[47] for the Col$_r$ phase, which exhibit a broad distribution of θ' angles between 0 and 25°, with a maximum at 15°. The observation of the section Absorption Spectra, that the absorption spectrum of $H_2Pc1410$ liquid crystal resembles that of α-H_2Pc crystals ($\theta' = 26.5°$) rather than that of β-H_2Pc crystals ($\theta' = 46.8°$), also indicates that θ' must be quite small. Grazing incidence X-ray scattering for thin films[48] yields a θ'' angle (between stack and normal to the surface) of 17°, in agreement with previous literature.[9] All θ angles between $|\theta' - \theta''| \approx 0°$ and $|\theta' + \theta''| \approx 32°$ would be possible in the absence of correlation between θ' and θ''. For this reason, the finding that the allowed values of θ are well below the maximum possible angle $|\theta' + \theta''|$ indicates that θ' and θ'' are highly correlated and tend to compensate each other, yielding an arrangement in which the molecular cores are, on average, approximately parallel to surface, as first stated in ref 48.

CONCLUSIONS

The aggregates of the phthalocyanine derivative $H_2Pc1410$ in the homeotropic LC phase are found to display a broad emission red-shifted with respect to the one of the monomeric species. Both point dipole exciton theory by Kasha[13] and the coupled oscillator model by Förster[49] predict that in perfectly stacked face to face aggregates the fluorescence quantum yield should be

negligible. However, a relaxation of the selection rules is probably made possible by the flexibility of the $H_2Pc1410$ columnar arrangement in the LC, which results in a wide distribution of the relative orientations of the phthalocyanine cores. The appearance of a monomeric emission under irradiation suggests that localized heating may induce the formation of disordered domains.

Polarized Raman measurements, supported by a theoretical description of the band intensities in an oriented sample, confirm and verify the alignment, also detected by other techniques, in the homeotropic samples. This approach also succeeds in constraining the possible values of the tilt angle θ which measures the alignment of the flat molecular disks with respect to the substrate. While the results of this work are consistent with previous studies,[1,9,48] it is certainly worth pointing out how polarization Raman spectroscopy can be used as a quick and effective tool to check the degree of order in these systems.

ASSOCIATED CONTENT

S **Supporting Information.** Mathematica code used to compute the Raman intensities. This material is available free of charge via the Internet at http://pubs.acs.org.

AUTHOR INFORMATION

Corresponding Author
*E-mail: elisabetta.venuti@unibo.it.

ACKNOWLEDGMENT

REFERENCES

(1) Tant, J.; Geerts, Y. H.; Lehmann, M.; De Cupere, V.; Zucchi, G.; Laursen, B. W.; Bjornholm, T.; Lemaur, V.; Marcq, V.; Burquel, A.; Hennebicq, E.; Gardebien, F.; Viville, P.; Beljonne, D.; Lazzaroni, R.; Cornil, J. *J. Phys. Chem. B* **2005**, *109*, 20315–20323.

(2) Hatsusaka, K.; Ohta, K.; Yamamoto, I.; Shirai, H. *J. Mater. Chem.* **2001**, *11*, 423–433.

(3) Nolte, R. J. M. *Liq. Cryst.* **2006**, *33*, 1373–1377.

(4) Tracz, A.; Makowski, T.; Masirek, S.; Pisula, W.; Geerts, Y. H. *Nanotechnology* **2007**, *18*, 485303/1–5.

(5) Claessen, C. G.; Hahn, U.; Torres, T. *Chem. Rec.* **2008**, *8*, 75–97.

(6) De Cupere, V.; Tant, J.; Viville, P.; Lazzaroni, R.; Osikowicz, W.; Salaneck, W. R.; Geerts, Y. H. *Langmuir* **2006**, *22*, 7798–7806.

(7) Bushby, R. J. U.; Lozman, O. R. *Curr. Opin. Colloid Interface Sci.* **2002**, *7*, 343–354.

(8) Kaafarani, B. R. *Chem. Mater.* **2011**, *23*, 378–396.

(9) Gearba, R. I.; Bondar, A. I.; Goderis, B.; Bras, W.; Ivanov, D. A. *Chem. Mater.* **2005**, *17*, 2825–2832.

(10) Deibel, C.; Janssen, D.; Heremans, P.; De Cupere, V.; Geerts, Y.; Benkhedir, M. L.; Adriaenssens, G. J. *Org. Electron.* **2006**, *7*, 495–499.

(11) Cavallini, M.; Calò, A.; Stoliar, P.; Kengne, J. C.; Martins, S.; Matacotta, F. C.; Quist, F.; Gbabode, G.; Dumont, N.; Geerts, Y. H.; Biscarini, F. *Adv. Mater.* **2009**, *21*, 4688–4691.

(12) Schweicher, G.; Gbabode, G.; Quist, F.; Debever, O.; Dumont, N.; Sergeyev, S.; Geerts, Y. H. *Chem. Mater.* **2009**, *21*, 5867–5874.

(13) Kasha, M.; Rawls, H. R.; Ashraf El-Bayoumi, M. *Pure Appl. Chem.* **1965**, *11*, 371–392.

(14) Pope, M.; Swenberg, C. E. *Electronic Processes in Organic Crystals*; Oxford University Press: New York, 1982.

(15) Beljonne, D.; Cornil, J.; Silbey, R.; Milliè, P.; Brédas, J. L. *J. Chem. Phys.* **2000**, *112*, 4749–4758.

(16) Markovitsi, D.; Gallos, L. K.; Lemaistre, J. P.; Argyrakis, P. *Chem. Phys.* **2001**, *269*, 147–158.

(17) Fitzgerald, S.; Farren, C.; Stanley, C. F.; Beeby, A.; Bryce, M. R. *Photochem. Photobiol. Sci.* **2002**, *1*, 581–587.

(18) Freyer, W.; Neacsua, C. C.; Raschkeb, M. B. *J. Lumin.* **2008**, *128*, 661–672.

(19) Tackley, D. R.; Dent, G.; Smith, W. E. *Phys. Chem. Chem. Phys.* **2001**, *3*, 1419–1426.

(20) Frisch, M. J.; Trucks, G. W.; Schlegel, H. B.; Scuseria, G. E.; Robb, M. A.; Cheeseman, J. R.; Montgomery, J. A., Jr.; Vreven, T.; Kudin, K. N.; Burant, J. C.; Millam, J. M.; Iyengar, S. S.; Tomasi, J.; Barone, V.; Mennucci, B.; Cossi, M.; Scalmani, G.; Rega, N.; Petersson, G. A.; Nakatsuji, H.; Hada, M.; Ehara, M.; Toyota, K.; Fukuda, R.; Hasegawa, J.; Ishida, M.; Nakajima, T.; Honda, Y.; Kitao, O.; Nakai, H.; Klene, M.; Li, X.; Knox, J. E.; Hratchian, H. P.; Cross, J. B.; Bakken, V.; Adamo, C.; Jaramillo, J.; Gomperts, R.; Stratmann, R. E.; Yazyev, O.; Austin, A. J.; Cammi, R.; Pomelli, C.; Ochterski, J. W.; Ayala, P. Y.; Morokuma, K.; Voth, G. A.; Salvador, P.; Dannenberg, J. J.; Zakrzewski, V. G.; Dapprich, S.; Daniels, A. D.; Strain, M. C.; Farkas, O.; Malick, D. K.; Rabuck, A. D.; Raghavachari, K.; Foresman, J. B.; Ortiz, J. V.; Cui, Q.; Baboul, A. G.; Clifford, S.; Cioslowski, J.; Stefanov, B. B.; Liu, G.; Liashenko, A.; Piskorz, P.; Komaromi, I.; Martin, R. L.; Fox, D. J.; Keith, T.; Al-Laham, M. A.; Peng, C. Y.; Nanayakkara, A.; Challacombe, M.; Gill, P. M. W.; Johnson, B.; Chen, W.; Wong, M. W.; Gonzalez, C.; Pople, J. A. *Gaussian03*, revision D.02; Gaussian, Inc.: Wallingford CT, 2004.

(21) Scott, A. P.; Radom, L. *J. Phys. Chem.* **1996**, *100*, 16502–16513.

(22) Lee, C.; Yang, W.; Parr, R. G. *Phys. Rev. B* **1988**, *37*, 785–789.

(23) Merrick, J. P.; Moran, D.; Radom, L. *J. Phys. Chem. A* **2007**, *111*, 11683–11700.

(24) Polavarapu, P. L. *J. Phys. Chem.* **1990**, *94*, 8106–8112.

(25) Wilson, E. B.; Decius, J. C.; Cross, P. C., *Molecular Vibrations*; McGraw-Hill: New York, 1955.

(26) Goldstein, H. *Classical Mechanics*; Addison-Wesley: Reading, MA, 1981.

(27) The Mathematica code used to compute the Raman intensities is provided as part of the Supporting Information. The rotation matrix $\mathbf{R}(\psi,\theta,\phi)$ is given in the code.

(28) Michalska, D.; Wysokinski, R. *Chem. Phys. Lett.* **2005**, *403*, 211–217.

(29) Kraulis, P. J. *J. Appl. Crystallogr.* **1991**, *24*, 946–950.

(30) Van Mingroot, H.; De Backer, S.; van Stam, J.; Van der Auweraer, M.; De Schryver, F. C. *Chem. Phys. Lett.* **1996**, *253*, 397–402.

(31) Kobayashi, N.; Ogata, H.; Nonaka, N.; Luk'Janets, E. A. *Chem.—Eur. J.* **2003**, *9*, 5123–5134.

(32) Duzhko, V.; Singer, K. D. *J. Phys. Chem. C* **2007**, *111*, 27–31.

(33) Schutte, W. J.; Sluyters-Rehbach, M.; Sluyters, J. H. *J. Phys. Chem.* **1993**, *97*, 6069–6073.

(34) Bayliss, S. M.; Heutz, S.; Rumbles, G.; Jones, T. S. *Phys. Chem. Chem. Phys.* **1999**, *1*, 3673–3676.

(35) Gould, R. D. *Coord. Chem. Rev.* **1996**, *156*, 237–274.

(36) Heutz, S.; Jones, T. S. *J. Appl. Phys.* **2002**, *92*, 3039–3046.

(37) Blasse, G.; Dirksen, G. J.; Meijerink, A.; van Der Pol, J. F.; Neeleman, E.; Drenth, W. *Chem. Phys. Lett.* **1989**, *154*, 420–424.

(38) Blanzat, B.; Barthou, C.; Tercier, N.; Andrè, J.-J.; Simon, J. *J. Am. Chem. Soc.* **1987**, *109*, 6193–6194.

(39) Sakakibara, Y.; Bera, R. N.; Mizutani, T.; Ishida, K.; Tokumoto, M.; Tani, T. *J. Phys. Chem. B* **2001**, *105*, 1547–1553.

(40) Aroca, R.; DiLella, D. P.; Loutfy, R. O. *J. Phys. Chem. Solids* **1982**, *43*, 707–711.

(41) Aroca, R.; Jennings, C.; Loutfy, R. O.; Hor, A.-M. *J. Phys. Chem.* **1986**, *90*, 5255–5257.

(42) Aroca, R.; Thedchanamoorthy, A. *Chem. Mater.* **1995**, *7*, 69–74.

(43) Heutz, S.; Salvan, G.; Silaghi, S. D.; Jones, T. S.; Zahn, D. R. T. *J. Phys. Chem. B* **2003**, *107*, 3782–3788.

(44) Basova, T. V.; Kolesov, B. A. *Thin Solid Films* **1998**, *325*, 140–144.

(45) Basova, T. V.; Durmus, M.; Gürek, A. G.; Ahsen, V.; Hassan, A. *J. Phys. Chem. C* **2009**, *113*, 19251–19257.

(46) Wolfram, S. *The Mathematica Book*; Wolfram Media: Champaign, IL, 2003.

(47) Olivier, Y.; Muccioli, L.; Lemaur, V.; Geerts, Y. H.; Zannoni, C.; Cornil, J. *J. Phys. Chem. B* **2009**, *113*, 14102–14111.

(48) Pouzet, E.; De Cupere, V.; Heintz, C.; Andreasen, J. W.; Breiby, D. W.; Nielsen, M. M.; Viville, P.; Lazzaroni, R.; Gbabode, G.; Geerts, Y. H. *J. Phys. Chem. C* **2009**, *113*, 14398–14406.

(49) Förster, T. *Naturwissenschaften* **1946**, *33*, 166–175.